

THE MOST VIOLENT SUPER-ACTIVE REGIONS IN THE 22ND AND 23RD CYCLES

LIRONG TIAN¹, YANG LIU² and JINXIU WANG¹

¹National Astronomical Observatories, Chinese Academy of Sciences, Beijing, 100012, China
(E-mail: tlr@ns.bao.ac.cn)

²W. W. Hansen Experimental Physics Lab., Stanford University, Stanford, CA 94305-4085, U.S.A.

(Received 15 March 2002; accepted 17 June 2002)

Abstract. We survey 14 super-active regions (SARs) in the 22nd cycle and 15 SARs in the 23rd cycle. Each produced major flares and major solar storms. Among them, the 25 most violent super active regions (VSARs) are selected based on five parameters: the largest area of sunspots, X-ray flare index (XRI), 10.7 cm radio flux, proton flux and geomagnetic A_p index. In order to understand the VSARs, we have investigated a few key magnetic properties of those regions, i.e., net magnetic flux, tilt angle and force-free parameter α_{best} . The following results are found: (1) Most VSARs (84%) in our samples have net magnetic flux greater than 10^{21} Mx, implying that those are seriously unbalanced flux regions. Unbalanced flux active regions probably provide a nest to relate the small-scale to the large-scale magnetic field. (2) Most of the VSARs (68%) are of abnormal magnetic structure, violating the Hale–Nicholson Law. For most of the normal VSARs, the tilt angles are larger than 40° . 84% of the VSARs follow the hemispheric helicity rule. Generally, they have large magnetic twist and writhe helicity. (3) We also enlarge our samples to study the locations of VSARs by adding the top 10 of the major flares, proton events and severe magnetic storms from 1976 to 2001. It is found that 77% in our 30 samples of VSARs were preferentially located in 4 longitude bands, i.e., $l_c = 80^\circ \pm 15^\circ$; $l_c = 170^\circ \pm 15^\circ$; $l_c = 260^\circ \pm 15^\circ$; and $l_c = 350^\circ \pm 15^\circ$. The interval of those longitude bands is roughly 90° . From the above results, we suggest that there probably is a special magnetic environment in the sub-photosphere of the four longitude bands where it is preferred to produce abnormal and complex active regions which easily produce major flares and major solar storms. Area, magnetic class, net magnetic flux, Carrington longitude and tilt angle of an active region may serve to predict likelihood of the active region producing hazardous space weather.

1. Introduction

It is important to understand the solar sources of space weather hazards at Earth's orbit. Now, it is believed that Coronal Mass Ejections (CMEs) play the primary role in producing disastrous 'space weather' because energetic particles produced by CMEs can enhance radiation belts and cause geomagnetic storms and sun-storms, disturbing fields, and current systems. The causes and origins of CMEs remain among the outstanding questions in space physics. The observations of CMEs by LASCO coronagraphs on board SOHO suggest that there are two distinct types of CMEs (Andrews and Howard, 2001). The Type A (Acceleration) events are usually associated with prominence eruptions or filament disappearance (70%) (Munro *et al.*, 1979; Webb and Hundhausen, 1987) and the Type C (constant speed) events



are usually associated with long-duration X-ray flares. It is likely that both CMEs and flares arise from instabilities connected with the evolution of the magnetic field in the solar atmosphere. CMEs probably result more from changes in the large-scale magnetic field that permeates the solar corona and flares probably result from changes in the stronger but smaller scale fields associated with sunspot regions lower in the solar atmosphere.

Sudden release of energy stored in magnetic fields produces radiation from longest wavelength radio waves to shortest gamma rays and also releases energetic particles, which affect ionosphere and radio communication at Earth. Soft X-ray emission can be detected in the stage of release of magnetic energy. The radiation observed at soft X-ray energies is typically originated from thermal plasma with a temperature in the order of 10–30 million deg Kelvin. The X-ray flare index (XRI) is a value as a measure of this short-lived activity on the Sun. This index is the sum of the numerical multipliers of the X-ray flare classes M and X for the disk transit of the active regions with M1 flares counting 0.1, M2 as 0.2; X1 flares as 1.0, etc.

It is well known that δ -sunspots are highly active in producing energetic flares (Zirin, 1988; Shi and Wang, 1994). Sammis, Tang, and Zirin (2000) confirmed Kunzel's idea (1960) that regions classified $\beta\gamma\delta$ produced many more large flares than other regions of comparable size and each region larger than $1000 \mu\text{h}$ and classified $\beta\gamma\delta$ had nearly 40% probability of producing flares classified X1 or greater. Greatrix (1963) in a comprehensive statistical analysis covering two separate periods, found that flare frequency is a linear function of spot area. Achong, Stahl, and Nyack (1982) further examined the degree of associated geo-effective SID (Sudden Ionospheric Disturbance) flares and sunspot morphology. They concluded that the probability of a sunspot group being magnetically complex is a linear function of spot area. The larger this area is, the most likely a group is in the $\beta\gamma\delta$ magnetic class.

Solar flux at 10.7 cm comes from active region emissions with free-free and geo-magnetic mechanisms, a component which is sensitive to the magnetic fields, density and temperature above sunspots (Alissandrakis, 1980). The 10.7 cm solar flux is almost completely thermal in origin, and directly related to the total amount of plasma trapped in the magnetic fields overlying active regions. This in turn relates to the amount of magnetic flux. Energetic protons can reach the Earth within 30 min of a major flare peak. Recently it was suggested that there are two types of highly solar energy particles (SEP) (primarily protons) events (Reames, 1995; Cane, 1997). One is generated during solar flares, and the other, known as gradual SEP events for their time scales of days, are closely associated with fast ($v > 400 \text{ km s}^{-1}$) CMEs that drive coronal and interplanetary shocks (Kahler, 1996; Cane, 1997).

Geomagnetic disturbances can be monitored by ground-based magnetic observatories recording the three magnetic field components. Proton flux is an important factor in producing geomagnetic storms. A_p index is the planetary index for measuring the strength of a disturbance in the Earth's magnetic field, defined over a

period of one from a set of standard stations around the world. A storm occurs when the $A_p > 29$. Storms are classified into three levels, minor storms when $29 \leq A_p < 50$, major storms when $50 \leq A_p \leq 100$ and severe storms when $A_p \geq 100$.

It is important to know which active regions are most likely to produce major flares and associate with CMEs, which kinds of active regions could make space weather hazards, and what observations are needed to predict CMEs-space weather hazards. This knowledge is certainly of great help for space weather prediction. Intensity of a solar cycle is characterized by a few of the strongest super-active regions (SARs). SARs were defined by Bai (1988) as active regions producing four or more major flares. In this paper, we pay attention to magnetic characteristics of the SARs which produced major X-ray flares with major solar storms in the 22nd and 23rd cycles by surveying three solar parameters (the largest area of sunspots, XRI and 10.7 cm peak flux) and two geomagnetic effect parameters (proton flux and A_p index). Then we search for the causes and origins to produce major solar storms. The structure of this paper is as following. In Section 2 we describe the data used and samples selected. The characteristics of those chosen active regions are presented in Sections 3–5. Our discussions and conclusions are in Section 6.

2. Data and Samples

The data used in this paper are the line-of-sight and transverse magnetograms in the photosphere taken by the Solar Magnetic Field Telescope at Huairou Solar Observatory Station (HSOS) and the line-of-sight magnetograms in the 23rd cycle from MDI aboard SOHO, the largest area of the sunspots, X-ray flare index (XRI), 10.7 cm peak flux, proton flux, and geomagnetic A_p index from NOAA and NASA web sites at <http://www.sec.noaa.gov> and <http://umbra.nascom.nasa.gov>, and from *Solar Geophysical Data (SGD)*.

The solar magnetic field telescope is a filter-type polarimeter. It works at the Fe I 5324.19 Å spectral line. The Stokes V is measured at -0.075 Å from the line center, and Q and U are taken at the line center. The field of view is 5.23 arc min \times 3.63 arc min (512 \times 512 pixels of CCD) and the data used are usually reduced to 2 arc sec \times 2 arc sec per pixel. Both theoretical and empirical methods are used to calibrate the vector magnetograms. Here, we use the force-free approximation to remove the 180° ambiguity. The noise level of the line-of-sight magnetic field is about 10 G for magnetograms integrated 256 frames. For the transverse field measurements, the noise level is estimated from the standard deviation of transverse field and is found about 100 G. More detailed description of observation and data reduction can be found in a paper by Wang *et al.* (1996).

In this paper, we choose 29 active regions that produced major flares and/or major solar storms. Among them 14 active regions are in the 22nd cycle and 15 active regions are in the 23rd cycle. Vector magnetic fields of those regions were acquired

in satisfactory weather when active regions were close to central meridian (-15° to 15°). Using the best magnetograms, we calculated magnetic flux, tilt angles and current helicity of the active regions. The projection effects of high-latitude active regions were removed using the formulae given by Gary and Hagyard (1990).

3. Super-Active Regions in the 22nd and 23rd Cycles

Tables I and II show information of super-active regions (SARs) studied in this paper. All the super-active regions survived during their disk passage so that quite good data coverages are available. Most SARs have $\beta\gamma\delta$ type magnetic structure. From these two tables, we find that the SARs with larger areas have generally produced larger flares and most of them have also produced severe solar storms and proton events, such as NOAA 6555, 6659, 5395, 5629, 5747, 5698, 6891, 7321, 6022, 6063, 9393, 9077, and 8100. This is in good agreement with the previous results by Sammis, Tang, and Zirin (2000), who confirmed that larger active regions have more major flares than small ones and also tend to be more complex. Therefore, the scale offered by large spots is an important index of an active region of producing great solar flares and storms. But, it is less significant than the dependence on magnetic class. We call such active regions, which have large spot area with magnetic class of $\beta\gamma\delta$ and produced major flares and great solar storms, as ‘the first kind of SARs’. Active regions with middle or smaller area, however, producing major flare and/or solar storms, are called as ‘the second kind of SARs’.

Comparing the two tables, we find that the first kind of the SARs in the 22nd cycle are obviously more than that in the 23rd cycle. While, in the 23rd cycle, more major solar storms are produced by the second kind of SARs. They are NOAA 9415, 9236, 8307, 9684, 9632, 9704, 8340, 9026, 8210 in the 23rd cycle and NOAA 5800, 7154, 6703, and 7671 in the 22nd cycle. XRIs of many SARs are smaller (except AR 9415, 9236, and 8307), but major solar storms. We should pay attention to this kind of the SARs in our prediction and search for the reasons that produce major solar storms because they are usually ignored due to small area.

4. Magnetic Flux and Property of Twist and Writhe of the Most Violent Super-Active Regions

We would like to call the SARs the most violent super-active regions (VSARs) if three of five parameters of the SARs, the largest area, XRI, 10.7 cm peak flux, proton flux and geomagnetic index A_p , are satisfied following criteria that (1) the largest area of sunspots is larger than $1000 \mu\text{h}$ (expressed in 10^{-6} solar hemisphere); (2) XRI is larger than 5.0; (3) 10.7 cm peak flux is more than 1000 s.f.u.; (4) proton flux ($> 10 \text{ Mev}$) is more than 400 p.f.u. and (5) geomagnetic index A_p

TABLE I
Super-active regions in the 22nd cycle.

NOAA	Lat. Long.	Date on the disk Y M D	Area, MC. (μ h)	X-ray flare index	10.7 cm peak flux (s.f.u.)	Proton flux (p.f.u.) (> 10 Mev)	Geo- mag. A_p
6555	S23 L186	910318-0331	2530 $\beta\gamma\delta$	32.6	36 000	43 000	165
6659	N31 L248	910602-0615	2300 $\beta\gamma\delta$	86.5	55 000	3000 1400	196
5395	N33 L260	890306-0319	3570 $\beta\gamma\delta$	57.0	18 000	3500 2000	250
5629	S17 L076	890803-0817	1320 $\beta\gamma\delta$	30.0	16 000	9200	80
5747	S27 L211	891014-1028	1160 $\beta\gamma\delta$	24.1	22 000	40 000 8300 4100	153
5698	S26 L220	890916-0930	1210 $\beta\gamma\delta$	9.8	2800	4500	73
6891	S12 L185	911011-1105	2570 $\beta\gamma\delta$	14.3	5300	40 94	130
7321	S24 L071	921024-1101	1650 $\beta\gamma\delta$	10.7	7700	2700 790	32
6022	N33 L345	900414-0427	1070 $\beta\gamma\delta$	1.4	11 000	12	125
6063	N34 L321	900513-0524	940 $\beta\gamma\delta$	23.1	13 000	410 180	30
5800	N25 L080	891119-1202	590 $\beta\gamma$	3.6	2100	7300 380	110
7154	S28 L157	920504-0515	500 β	2.1	3100	4600	180
6703	N26 L239	910628-0713	280 $\beta\gamma$	1.9	1778	2300 110	135
7671	N11 L188	940213-0226	450 β	1.7	190	10 000	95

is larger than 50. With these criteria, 13 SARs in the 22nd cycle and 12 SARs in the 23rd cycle are selected as VSARs. They are AR 6555, 6659, 5395, 5629, 5747, 5698, 6891, 7321, 6022, 6063, 5800, 7154, 6703; AR 9393, 9077, 9415, 9236, 8307, 9684, 9632, 9704, 8340, 9026, 8210, and 8100 in Tables I and II. In the following, we will investigate some properties of the VSARs.

4.1. TOTAL AND NET MAGNETIC FLUX OF THE VSARS

It is necessary to study the local and global magnetic field and interactions between them in order to understand the mechanisms of major solar flares and severe solar storms. To this purpose, we search for net flux of the VSARs selected above. In

TABLE II
Super-active regions in the 23rd cycle.

NOAA	Lat. Long.	Date on the disk Y M D	Area, MC. (μ h)	X-ray flare index	10.7 cm peak flux (s.f.u.)	Proton flux (p.f.u.) (>10 Mev)	Geo- mag. mag. A_p
9393	N17 L151	010323-0405	2440 $\beta\gamma\delta$	27.0 3X25M	10 000	1110	192
9077	N18 L310	000708-0721	1010 $\beta\gamma\delta$	11.7 3X11M	2600	24 000	164
9415	S22 L001	010403-0416	880 $\beta\gamma\delta$	28.9 6X8M	48 000	951	87
9236	N20 L352	001118-1130	630 $\beta\gamma\delta$	12.8 5X3M	2200	942	52
8307	N31 L038	980819-0901	570 $\beta\gamma\delta$	15.7 5X7M	2400 2100	665	145
9684	N06 L136	011028-1108	550 $\beta\gamma\delta$	1.2 1X1M	1900	31 000 24 300	112
9632	S19 L272	010920-0930	790 $\beta\gamma\delta$	2.8 1X2M	7500	12 900	73
9704	S18 L271	011115-1127	610 $\beta\gamma\delta$	2.5 1X3M	9700	18 900	108
8340	N20 L013	980918-0930	540 $\beta\gamma\delta$	0.8 1M	1100	1200	117
9026	N21 L074	000601-0614	910 $\beta\gamma\delta$	8.4 3X8M	2300	84	65
8210	S21 L140	980425-0508	480 $\beta\gamma\delta$	7.9 6X4M	1000	150 210	101
8100	S20 L351	971027-1108	3300 $\beta\gamma\delta$	12.7 2X5M	690	490 72	44
9661	N15 L357	011011-1022	800 $\beta\gamma\delta$	3.5 2X2M	1400	24 16	66
8375	N18 L182	981030-1111	720 $\beta\gamma\delta$	1.7 6M	400	310	76
9682	N12 L173	011025-1105	1210 $\beta\gamma\delta$	1.9 10M	180	1850	41
8765	S13 L236	991112-1122	1280 $\beta\gamma\delta$	2.0 9M	340	0	43

principle, the amount of magnetic flux of the positive concentration should balance that of the negative one. In reality, however, emerging flux is often unbalanced. Because unbalanced flux active regions can provide a nest to relate the small-scale to the large-scale magnetic field, instability of magnetic field in the small-scale field can affect the large-scale magnetic field and eventually induce loss of stability in large-scale field and cause CMEs.

Table III shows the properties of the first type of the VSARs with large area and producing major solar flares and major solar storms; and Table IV lists the second type of the VSARs with middle and little area and producing major solar storms, but small (sometimes large) XRI. In these tables, the total magnetic flux is defined as absolute sum of the positive and negative fluxes above the noise level. The net flux is the difference between them. They are calculated when the VSARs were near the solar disk center.

In Tables III and IV, 84% of the VSARs have net magnetic flux higher than 10^{21} Mx. Apparently, the active regions that produce major solar storms are in seriously unbalanced-flux situations. The more the total flux and net flux are, the larger the solar flares and solar storms are. Thus, unbalanced-flux active regions are likely to generate large-scale activities such as major solar storms. Liu and Andrews (2001) studied the relationship between coronal mass ejections and unbalanced-flux active regions, including NOAA 9077, 9236, 8210, and 8100. They found that those regions have trans-equator loops or a large-scale loop connecting to polar region, seen in *Yohkoh* SXT images. These large-scale magnetic systems connect those unbalanced-flux regions to remote parts. Therefore, net magnetic flux of an active region would be an index for predicting CMEs and solar storms.

4.2. THE TWIST OF MAGNETIC FIELD OF THE VSARS

Magnetic fields of active regions are commonly non-potential. The non-potentiality of the magnetic fields can be demonstrated by force-free parameter α_{best} calculated in the photosphere (Pevtsov, Canfield, and Metcalf, 1995). It shows the twist of magnetic lines. Positive/negative values of this parameter correspond to twist of right/left-handedness. On the whole, the value could describe the complexity of magnetic field in active regions. Observation reveals the dominance of negative/positive helicity in the northern/southern hemisphere, which is called the ‘rule of helicity sign’.

We computed the force-free parameter α_{best} of the 25 VSARs when active regions were near solar disk center and magnetic fields are above noise level. They are listed in Tables III and IV. Those values are an average from three best vector magnetograms in the same day. It is found that most (84% of 25) VSARs have normal twist following the rule of helicity sign, and 76% of them have a force-free parameter α_{best} larger than 0.04 Mm^{-1} . This suggests that most active regions are much more complex in small-scale, in agreement with the magnetic class of $\beta\gamma\delta$.

TABLE III
Magnetic flux, twist, and writhe of the first kind of VSARs.

NOAA	Lat. Long.	Total flux (10^{22} Mx)	Net flux (10^{22} Mx)	α_{best} (Mm^{-1})	Twist (handedness)	Tilt angle (deg)	Writhe (handedness)
6555	S23 L186	3.84	-1.75	0.047 (normal)	right	-24.5 (abnormal)	right
6659	N31 L248	3.32	-1.53	-0.083 (normal)	left	59.4 (normal)	right
5395	N33 L260	3.97	+1.50	-0.175 (normal)	left	83.4 (normal)	right
5629	S17 L076	6.24	+1.65	0.081 (normal)	right	-110.9 (abnormal)	right
5747	S27 L211	2.18	-0.32	-0.075 (abnormal)	left	-48.9 (abnormal)	right
5698	S26 L220	2.02	+0.01	0.147 (normal)	right	52.2 (normal)	left
6891	S12 L185	7.71	+1.45	0.043 (normal)	right	46.5 (normal)	left
7321	S24 L071	2.93	+0.13	0.063 (normal)	right	-58.6 (abnormal)	right
9393	N17 L151	5.96	+1.2	-0.016 (normal)	left	-65.5 (abnormal)	left
9077	N18 L310	3.33	-0.37	0.081 (normal)	left	-53.0 (abnormal)	left
8100	S20 L351	1.46	-0.02	-0.017 (abnormal)	left	24.6 (normal)	left
6063	N34 L321	1.78	+0.95	-0.05 (normal)	left	44.1 (normal)	right
6022	N33 L345	1.17	+0.25	-0.47 (normal)	left	-85.3 (abnormal)	right

4.3. THE WRITHE OF MAGNETIC FIELD OF THE VSARS

The Hale–Nicholson law (Hale and Nicholson, 1938) states that in many bipolar magnetic fields, the magnetic polarity axis has a particular inclination, with the preceding spot closer to the solar equator than the following spot. The angle between the magnetic polarity axis and the solar equator is defined as the ‘tilt angle’. The physical origin of the tilt angle has been discussed by Babcock (1961), Schmidt (1968) and Wang and Sheeley (1991), who suggested that the tilts are formed by

TABLE IV
Magnetic flux, twist and writhe of the second kind of VSARs.

NOAA	Lat. Long.	Total flux (10^{22} Mx)	Net flux (10^{22} Mx)	α_{best} (Mm^{-1})	Twist (handedness)	Tilt angle (deg)	Writhe (handedness)
9684	N06 L136	2.41	+0.46	-0.027 (normal)	left	-32.7 (abnormal)	left
8210	S21 L140	1.89	+0.13	0.073 (normal)	right	143 (abnormal)	left
8340	N20 L013	2.34	-0.18	0.040 (abnormal)	right	-37.7 (abnormal)	left
9415	S22 L001	3.60	+0.30	0.170 (normal)	right	-59.5 (abnormal)	right
5800	N25 L080	1.53	+0.35	-0.119 (normal)	left	-21.2 (abnormal)	left
9236	N20 L352	2.65	+0.55	-0.022 (normal)	left	23.0 (normal)	right
7154	S28 L157	1.75	+0.33	-0.027 (abnormal)	left	7.2 (normal)	left
9632	S18 L271	2.55	-0.37	0.052 (normal)	right	-39.2 (abnormal)	right
9704	S18 L271	3.23	-0.35	0.056 (normal)	right	-81.4 (abnormal)	right
9026	N21 L074	2.55	+0.06	-0.014 (normal)	left	-31.6 (abnormal)	left
8307	N31 L038	1.26	-0.30	-0.050 (normal)	left	-22.5 (abnormal)	left
6703	N26 L239	0.83	-0.02	-0.117 (normal)	left	-129.7 (abnormal)	left

the Coriolis force acting on the expanding plasma contained within a buoyant, rising flux tube in sub-photosphere.

In calculations of the tilt angle (φ), the position of each magnetic polarity could be approximately indicated by the flux-weighted center of each main polarity in the line of sight. Here, introducing a separation vector ($\mathbf{r}_l - \mathbf{r}_f$) between the centers of the leading (l) and following (f) polarities in the heliographic plane, the tilt angle of an active region is defined as the angle between the vector and unit vector pointing from the west to east. We determinate that the sign of the tilt angle of active regions adhering to the Hale–Nicholson law is positive in interval of $0 < \varphi < 90$ deg. They are normal active regions. If the S/N (N/S) being leading polarity is closer to

the solar equator in the northern (southern) hemisphere, the tilt is positive in the 22nd/23rd cycles; otherwise a negative tilt and abnormal active region. The active regions with positive tilt angles are right/left-handed writhe of a flux tube in the northern/southern hemisphere.

The tilt angle approximately reflects the global direction of the magnetic field of an active region. According to the Hale–Nicholson law, the leading polarity of a bipolar should be preferentially located equatorward of its following polarity. From Tables III and IV, however, it is found that most active regions (68%) have negative tilt angles. As our convention of sign of the tilt angle, the 68% VSARs are abnormal active regions, much different from the active region orientation described by the Hale–Nicholson law. Others (8 VSARs) have positive tilt angle. However, five of them have larger than 40° and two have the same handedness between the twist and writhe of magnetic fields. This is obviously different from most simple bipolar active regions in which the tilt angles are commonly smaller than 30° and most active regions have opposite handedness between the twist and writhe of magnetic fields (Figures 2 and 3 in Tian *et al.*, 2001). It could indicate larger total helicity (sum of the twist and writhe helicity) because of the same handedness of the twist and writhe. Thus, as a whole, the magnetic structure of the active regions is complex in large-scale.

Therefore, we conclude that most VSARs are highly unbalanced-flux active regions which either violate the Hale–Nicholson law or have larger magnetic helicity.

5. Position of the VSARs in Heliographic Coordinates

When and where the major flares and severe solar storms will occur is an important topic to observers. Analysis of sunspot group formation or of sites of high flare production shows that there are preferred longitudes where these phenomena occur. It is useful for the prediction of solar activity.

Bai (1988) studied super-active regions in three solar cycles and found there were three ‘active zones’: $l_n = 40^\circ - 120^\circ$; $l_n = 185^\circ - 215^\circ$; $l_n = 270^\circ - 360^\circ$ in cycle 19 and two ‘active zones’: $l_n = 85^\circ - 145^\circ$ and $l_n = 270^\circ - 330^\circ$ during cycles 20 and 21; Dodson and Hedeman (1975) noticed that during 1970–1974 period there exist two active longitude bands centered around $l_c = 90^\circ$ and $l_c = 270^\circ$, and during the 1973–1974 period there exists only one active longitude band centered around $l_c = 180^\circ$; Švestka (1970) identified an active longitude band centered around $l_c = 180^\circ$ during 1963–1967.

Using the Carrington longitude l_c , we investigate the distribution of those VSARs selected in the 22nd and 23rd cycles. The ‘ \diamond ’ sign in Figure 1 denotes the VSARs. We found that these VSARs occurred in four active longitude bands: $l_c = 80^\circ \pm 15^\circ$; $l_c = 170^\circ \pm 15^\circ$; $l_c = 260^\circ \pm 15^\circ$; $l_c = 350^\circ \pm 15^\circ$. The spacing of each center of active longitude bands is about 90° . We also studied the active regions in the top 10 of major flares, top 10 of severe magnetic storms and the top

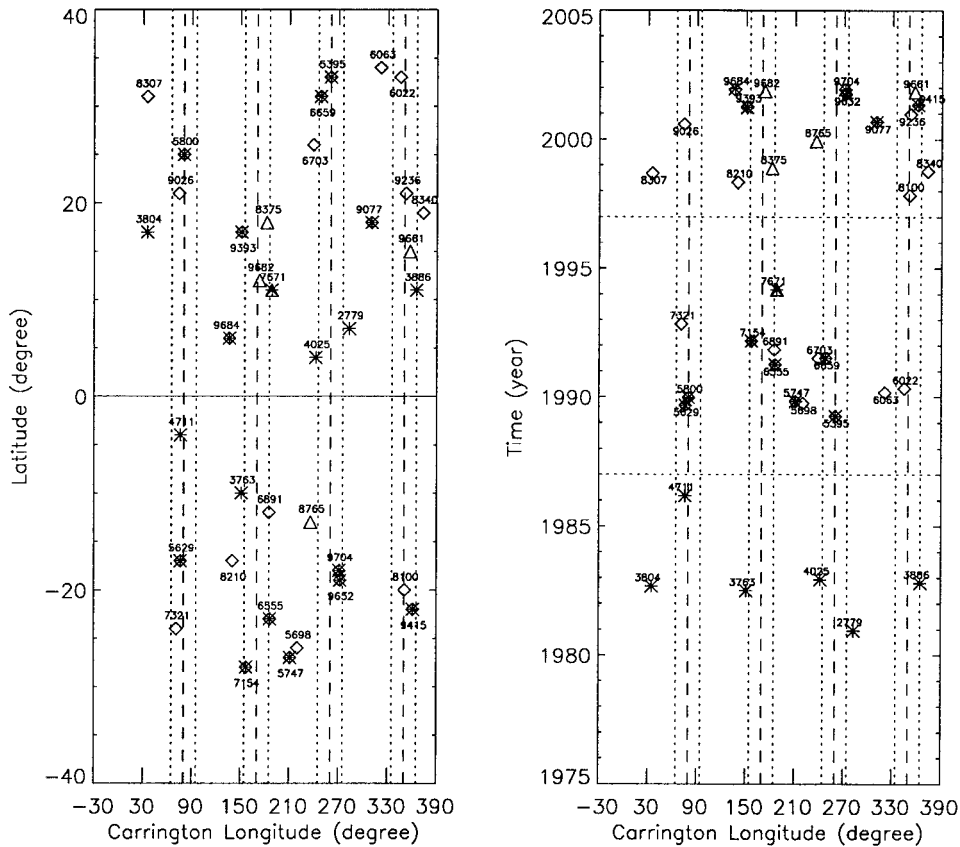


Figure 1. Position of the most violent super-active regions in heliographic coordinates. ‘◇’ denotes the VSARs selected by us. ‘*’ sign denotes the VSARs in top 10 of major flares, severe magnetic storms and proton events, respectively, from 1976 to 2001. Their information is shown in Table V. ‘△’ denotes SARs selected down. We need to note that real longitudes of NOAA 9415 and 8340 are L1 and L13, respectively. We add 360° to them in order to show near one of active longitude bands.

10 of proton events from 1976 to 2001 (see Table V). The ‘*’ symbol in Figure 1 denotes the active regions in the top 10 of major flares, proton events and solar storms from 1976 to 2001. They correspond to 20 super-active regions. ‘△’ denotes 5 SARs selected by us because of fitting only two or one of the five parameters as criteria. They are NOAA 9682, 9661, 8765, 8375, and 7671. However, NOAA 7671 is still one of VSARs because of being in the top 10 of proton events. We find that they were almost located in the four active longitude bands.

Thus, there are 32 VSARs in this study, shown using ‘◇’ and ‘*’ in Figure 1. However, NOAA 5698 and 5757, NOAA 9632 and 9704 are two recurrent pairs. Thus, of 30 different VSARs, only seven, NOAA 3804, 8307, 9684, 8210, 5747 (5698), 6063, and 9077, are a bit far from the four active longitude bands. Others (77%) are all in the four active longitude bands. This result is in good agreement

TABLE V

'Top ten' of the violent super-active regions from 1976 to 2001.

Major solar flares		Proton events		Severe magnetic storms	
NOAA	XRI	NOAA	P.f.u.	NOAA	A_p
6659	86.5	6555	43,000	5395	250
5395	57.0	5747	40,000	3804	229
3763	42.4	9684	31,700	4711	228
4025	36.7	9077	24,000	3886	201
6555	32.6	9704	18,900	6659	196
3804	31.4	9632	12,900	7154	193
5629	30.0	7671	10,000	9393	192
9415	28.9	5629	9,200	6555	165
9393	27.0	5800	7,300	9077	164
2779	25.9	7154	4,600	5747	153

with previous results studied by Bai (1988), Dodson and Hedeman (1975), and Švestka (1970). It is inferred that the four active longitude bands exist over a long period of time.

From the left panel in Figure 1, we find the distribution of the VSARs is asymmetric in southern and northern hemispheres. There are 18 VSARs (60%) in the northern hemisphere and 12 VSARs (40%) in the southern. From the right panel of Figure 1, we find the VSARs appeared repeatedly in each active longitude band at different times and in different solar cycles.

6. Conclusions and Discussion

Considering high and strong productivity of major flares and major solar storms related to some active regions, we call those 'the most violent super active regions' (VSARs). By studying net magnetic flux, tilt angle and twist of magnetic fields for the 25 VSARs in 22nd and 23rd cycles, we found the following results:

- (1) Most of these VSARs (84%) have larger net magnetic flux than 10^{21} Mx.
- (2) Most of the VSARs (68%) are of abnormal magnetic structure, violating the Hale–Nicholson law. For most of the normal VSARs, the tilt angles are larger than 40° . Eighty-four percent of the VSARs follow hemispheric helicity rule. Generally, they have large magnetic twist and writhe helicity.
- (3) Most of 30 VSARs (77%) from 1976 to 2001 are preferentially located in four active longitude bands: $l_c = 80^\circ \pm 15^\circ$; $l_c = 170^\circ \pm 15^\circ$; $l_c = 260^\circ \pm 15^\circ$; $l_c = 350^\circ \pm 15^\circ$. The spacing of each center of active longitude bands is about 90° .

From these results, we suggest that there probably is a special magnetic environment in sub-photosphere of the four active longitude bands where it is preferred to produce abnormal and complex active regions which easily produce major flares and major solar storms.

The averaged orientation of bipolar active regions is actually not quite toroidal; instead it is slightly tilted away from the azimuthal direction, with the leading polarity slightly closer to the equator than following polarity. The Coriolis force acts on the diverging velocity field of a rising flux-loop to writhe this loop into inverse-S shaped geometry (seen in projection from the top) in the northern hemisphere. However, the tilt angles of most active regions with simple magnetic structure are not larger than 30° (Tian *et al.*, 2001). If the tilt angle originating from the Coriolis force is large enough, the S or inverse-S shaped coronal loop will be so obvious that it can be seen in SXT images. Canfield, Hudson, and Pevtsov (2000) found approximately 60–70% of coronal loops are backward-S/S shaped in the northern/southern hemisphere. They showed that sigmoidal shape can be used as a reliable indicator of the likelihood that an active region will erupt. On this sense, the large tilt angle of an active region in the photosphere is a similar indicator predicting the possibility of eruption of the active region. From this result, we expect that the toroidal fields of active regions, described by the Hale–Nicholson polarity law, play an important role in geomagnetic storms. Thus, the magnetic structure of individual active regions plays a significant role in geomagnetic storms.

The reason that sunspot groups tend to form at favored longitudes is thought to be due to underlying magnetic fields. These fields control most phenomena on the sun, and observations have shown that they often tend to be long-lived, stable and appear repeatedly. It is thus reasonable that events controlled by these fields should occur at spatial positions relative to them. Combining the results obtained in this paper and previous results obtained by Bai (1988), Dodson and Hedeman (1975) and Švestka (1970), we suggest that there should be a special magnetic structure in the sub-photosphere of those active longitude bands. It lasts over a long-term period, over which major flares and major solar storms and hazardous space weather are produced repeatedly.

Area, magnetic class, net magnetic flux, Carrington longitude and tilt angle of an active region can probably serve as indexes to predict likelihood of the active region producing hazardous space weather.

Generally, big active regions have some tendency to be recurrent, such as NOAA 9704 (9632), 9393, 9026, 8645, 8307, and 8210 in the 23rd cycle and NOAA 6891, 6859, 6659, 5698 (5757), and 5629 in the 22nd cycle. These active regions should have some special characters, which will be studied in the following. In this study, the results are almost not changed, because there are only two pairs recurrent, NOAA 9704 (9632) and 5698 (5757), in our samples.

Acknowledgements

The authors thank the referee, Dr Axel Hofmann, for his valuable suggestions and comments. This research is supported by NSFC Grant 19973009 and NKBRSF G20000784 in China and Y. Liu was supported by NASA NAG5-3077. The authors are indebted to the TRACE, SOHO and SGD teams for providing wonderful data. They are grateful to the HSOS team for good observations of vector magnetic fields.

References

- Achong, A., Stahl, P. A., and Nyack, C.: 1982, *Solar Phys.* **88**, 137.
 Alissandrakis, C. E.: 1980, *Astron. Astrophys.* **82**, 30.
 Andrews, M. D. and Howard, R. A.: 2001, *Space Sci. Rev.* **95**, 147.
 Babcock, H. W.: 1961, *Astrophys. J.* **133**, 572.
 Bai, T.: 1988, *Astrophys. J.* **328**, 860.
 Cane, H. V.: 1997, in N. Crooker, J. Joselyn, and J. Feynman (eds.), *Coronal Mass Ejections*, p. 205.
 Canfield, R., Hudson, H., and Pevtsov, A.: 2000, *IEEE Trans. Plasma Sci.* **28**, 1786.
 Dodson, H. W. and Hedeman, E. R.: 1975, *Solar Phys.* **42**, 121.
 Gary, G. A. and Hagyard, M. J.: 1990, *Solar Phys.* 126, 21.
 Greatrix, G. R.: 1963, *Monthly Notices Royal. Astron. Soc.* **126**, 132.
 Hale, G. E. and Nicholson, S. B.: 1938, *Magnetic Observations of Sunspots, 1917–1924*, Carnegie Institute, Washington, DC.
 Kahler, S. W.: 1996, in R. Ramaty, N. Mandzhavidze, and X. Hua (eds.), *High Energy Solar Physics*, **374**, 61.
 Kunzel, H.: 1960, *Astron. Nachr.* **285**, 271.
 Liu, Y. and Andrews, M.: 2001, *AGU Summer Meeting* **41**, 11.
 Munro, R. H., Gosling, J. T., Hildner, E., MacQueen, R., Poland, A., and Rossi, C.: 1979, *Solar Phys.* **61**, 201.
 Pevtsov, A. A., Canfield, R. C., and Metcalf, T. R.: 1995, *Astrophys. J.* **440**, L109.
 Reames, D. V.: 1995, *Rev. Geophys. Suppl.* **33**, 585.
 Sammis, I., Tang, F., and Zirin, H.: 2000, *Astrophys. J.* **540**, 583.
 Schmidt, H. U.: 1968, in K. O. Kiepenheuer (ed.), 'Structure and Development of Solar Active Regions', *IAU Symp.* **35**, 95.
 Shi, Z. X. and Wang, J. X.: 1994, *Solar Phys.* **149**, 105.
Solar-Geophysical Data: 1988–1996 Part I and II, NOAA, Boulder.
 Švestka, Z.: 1970, *Space Res.* **10**, 797.
 Tian, L. R., Bao, S. D., Zhang, H. Q., and Wang, H. N.: 2001, *Astron. Astrophys.* **374**, 294.
 Wang, J., Shi Z., Wang H., and Lü Y.: 1996, *Astrophys. J.* **456**, 861.
 Wang, Y. M. and Sheeley, N. R.: 1989, *Solar Phys.* **124**, 81.
 Webb, D. F. and Hundhausen A. J.: 1987, *Solar Phys.* **108**, 344.
 Zirin, H.: 1988, *The Solar Atmosphere*, Cambridge University Press, Cambridge.